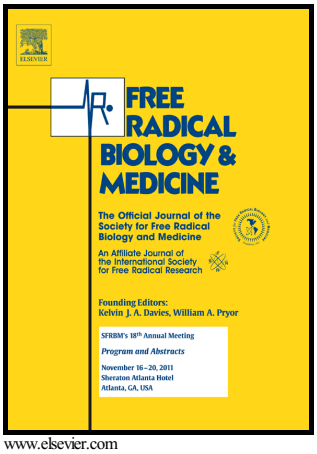

HYDROGEN PEROXIDE, NITRIC OXIDE AND ATP ARE MOLECULES INVOLVED IN CARDIAC MITOCHONDRIAL BIOGENESIS IN DIABETES

Silvina S. Bombicino, Darío E. Iglesias, Ivana A. Rukavina-Mikusic, Bruno Buchholz, Ricardo J. Gelpi, Alberto Boveris, Laura B. Valdez

PII: S0891-5849(17)30707-4
DOI: http://dx.doi.org/10.1016/j.freeradbiomed.2017.07.027
Reference: FRB13404

To appear in: *Free Radical Biology and Medicine*

Received date: 15 March 2017
Revised date: 12 July 2017
Accepted date: 25 July 2017

Cite this article as: Silvina S. Bombicino, Darío E. Iglesias, Ivana A. Rukavina Mikusic, Bruno Buchholz, Ricardo J. Gelpi, Alberto Boveris and Laura B Valdez, HYDROGEN PEROXIDE, NITRIC OXIDE AND ATP ARE MOLECULES INVOLVED IN CARDIAC MITOCHONDRIAL BIOGENESIS IN DIABETES, *Free Radical Biology and Medicine* http://dx.doi.org/10.1016/j.freeradbiomed.2017.07.027

HYDROGEN PEROXIDE, NITRIC OXIDE AND ATP ARE MOLECULES INVOLVED IN CARDIAC MITOCHONDRIAL BIOGENESIS IN DIABETES

Silvina S. Bombicino[1,3], Darío E. Iglesias[1,3], Ivana A. Rukavina-Mikusic[1,3], Bruno Buchholz[2,3], Ricardo J. Gelpi[2,3], Alberto Boveris[1,3], Laura B. Valdez[1,3*]

[1]University of Buenos Aires, School of Pharmacy and Biochemistry, Physical Chemistry Division. Buenos Aires, Argentina.

[2]University of Buenos Aires, Faculty of Medicine, Pathology Department, Cardiovascular Physiopathology Institute (INFICA).Buenos Aires, Argentina.

[3]Consejo Nacional de Investigaciones Científicas y Técnicas (CONICET), University of Buenos Aires, Institute of Biochemistry and Molecular Medicine (IBIMOL). Buenos Aires, Argentina.

[*]**Corresponding author.** Laura B. Valdez, Cátedra de Fisicoquímica, Facultad de Farmacia y Bioquímica, Universidad de Buenos Aires, Junín 956, C1113AAD, Buenos Aires, Argentina. Tel.: 54-11-5287-4235. E-mail: lbvaldez@ffyb.uba.ar

ABSTRACT

This study, in an experimental model of type I Diabetes Mellitus in rats, deals with the mitochondrial production rates and steady-state concentrations of H_2O_2 and NO, and ATP levels as part of a network of signaling molecules involved in heart mitochondrial biogenesis. Sustained hyperglycemia leads to a cardiac compromise against a work overload, in the absence of changes in resting cardiac performance and of heart hypertrophy. Diabetes was induced in male Wistar rats by a single dose of Streptozotocin (STZ, 60 mg×kg^{-1}, *ip.*). After 28 days of STZ-injection, rats were sacrificed and hearts were isolated. The mitochondrial mass (mg mitochondrial protein × g heart^{-1}), determined through cytochrome oxidase activity

ratio, was 47% higher in heart from diabetic than from control animals. Stereological analysis of cardiac tissue microphotographs showed an increase in the cytosolic volume occupied by mitochondria (30%) and in the number of mitochondria per unit area (52%), and a decrease in the mean area of each mitochondrion (23%) in diabetic respect to control rats. Additionally, an enhancement (76%) in PGC-1α expression was observed in cardiac tissue of diabetic animals. Moreover, heart mitochondrial H_2O_2 (127%) and NO (23%) productions and mtNOS expression (132%) were higher, while mitochondrial ATP production rate was lower (~40%), concomitantly with a partial-mitochondrial depolarization, in diabetic than in control rats. Changes in mitochondrial H_2O_2 and NO steady-state concentrations and an imbalance between cellular energy demand and mitochondrial energy transduction could be involved in the signaling pathways that lead to *the novo* synthesis of mitochondria. However, this compensatory mechanism triggered to restore the mitochondrial and tissue normal activities, did not lead to competent mitochondria capable of supplying the energetic demands in diabetic pathological conditions.

ABBREVIATIONS: DM, Diabetes Mellitus; mtNOS, Mitochondrial nitric oxide synthase; STZ , Streptozotocin; SOD, Superoxide dismutase; PCG-1α, Peroxisome proliferator-activated receptor-gamma coactivator

KEYWORDS: Heart mitochondria; Diabetes; Mitochondrial biogenesis; Mitochondrial nitric oxide synthase (mtNOS); Hydrogen peroxide; ATP.

1. INTRODUCTION

Mitochondria are the organelles that produce the energy required to drive the endergonic reactions of cell life and are part of the signaling process [1,2] involved in cellular division, differentiation, growth, aging and death. Additionally, mitochondria are the main cellular source of reactive oxygen species and also the target of their regulatory and toxic

actions. Superoxide anion ($O_2^{\bullet-}$) is formed through the autoxidation of ubisemiquinone [3,4] and of the flavinsemiquinone of NADH dehydrogenase [5], and it is disproportionated to hydrogen peroxide (H_2O_2) [6–8] by superoxide dismutase (SOD). Nitric oxide (NO) is biosynthesized in a reaction catalyzed by a nitric oxide synthase associated to the inner mitochondrial membrane (mtNOS) [9–11]. The recognition of a mitochondrial NOS activity in a series of organs with similar specific activities, the use of spectroscopic, electrochemical and fluorescent assays to detect NO production [12,13], the sequencing of liver mtNOS [14], and the dependence of mtNOS activity on metabolic state and membrane potential [15,16], strongly support both the recognition of mtNOS as a constitutive integral protein of the inner mitochondrial membrane and the concept that mitochondrial NO release is a physiological regulator of cytosolic and cellular functions [17]. Moreover, mtNOS is regulated by physiological effectors [18,19,16], by pharmacological treatments [20], and in pathological situations [21–25], being the product of its enzymatic activity, *i.e.* NO, an effective modulator of mitochondrial function through the inhibition that it exerts over complex IV [26–28] and complex III [29,30] activities. In addition, mtNOS structurally and/or functionally interacts with complex IV [31] and complex I proteins [24,32–35]. Nitric oxide is involved in S-nitrosation reactions of proteins and peptides [36,37] and gives rise to the formation of peroxynitrite ($ONOO^-$), a physiological nitrifying and oxidizing species [38–40].

At present, H_2O_2 and NO are considered mitochondrion-cytosol signaling molecules because they are involved in the modulation of redox-sensitive kinase signaling and transcriptional pathways [17,41–44]. H_2O_2 is considered as the major metabolite operative in redox sensing, signaling and redox regulation [45]. Steady-state concentration and spatial distribution of H_2O_2 in tissues is not uniform, existing substantial gradients between subcellular spaces [46,47]. Even within subcellular organelles, there are H_2O_2 gradients that produce “redox nanodomains”, which are induced by and control calcium signaling at the endoplasmic reticulum-mitochondrial interface [48]. In addition, changes in NO steady-state concentration have been associated with mitochondrial biogenesis [49–52], and increased $ONOO^-$ production has been involved in post-translational modifications of mitochondrial

proteins, such as complex I [17]. The biochemical communication between mitochondria and other subcellular components is considered essential in the regulation of the energy levels and the cellular redox homeostasis. The impairment of this mechanism seems to be inherent to the progression and/or pathological consequences of Diabetes [53,54].

Diabetes is characterized by an increase in blood glucose levels, being the hyperglycemia itself a well-recognized risk factor for developing heart failure [55]. This metabolic disease is typically accompanied by an increased production of free radicals and/or impaired antioxidants defense capabilities, indicating a central contribution of reactive oxygen and nitrogen species in the onset, progression and short- and long-term complications of Diabetes [56,57]. Results from our laboratory [58] have shown that sustained hyperglycemia leads to heart mitochondrial dysfunction, in which state 3 O_2 consumption and oxidative phosphorylation efficiency are decreased, leading to a cardiac compromise against a work overload. This mitochondrial impairment was observed in the absence of heart hypertrophy and of changes in resting cardiac performance, indicating that mitochondrial dysfunction precedes the onset of diabetic cardiac failure.

The aim of this work was to study heart mitochondrial biogenesis in relation to the production rates and steady-state concentrations of the mitochondrial molecules H_2O_2 and NO and to the energetic state (ATP level), in an experimental model of type I Diabetes Mellitus.

2. MATERIALS AND METHODS

2.1. Drugs and chemicals

Streptozotocin (STZ, S0130) and other chemicals were purchased from Sigma Chemical Co. (St. Louis, MO, USA). Anti-neuronal nitric oxide synthase antibodies (NOS 1, H299: cs-8309) and anti-PGC-1α (K 15: sc-5816) were from Santa Cruz Biotechnology (Santa Cruz, CA). Other reagents were of analytical grade.

2.2. Experimental design

Male Wistar rats of 6-7 weeks of age (200-220 g) were housed in separate cages in an environmentally controlled facility at 25 °C. The animals were subjected to circadian light–dark cycles, fed standard rat chow, and provided water *ad libitum*. The procedures used in this study were approved by the Animal Care and Research Committee of the School of Pharmacy and Biochemistry, University of Buenos Aires (CICUAL; 00663658/15), and this investigation was in accordance with the International Guiding Principles for Biomedical Involving Animals (ICLAS).

The experimental protocol have been previously utilized and published by Bombicino et. al [58]. Rats were divided in two groups, *Diabetes Mellitus* (DM) and *Control* (C). Diabetes was induced by a single dose of Streptozotocin (STZ, 60 mg $\times$ kg^{-1} animal weight, *i.p.*) diluted in citrate buffer 100 mM pH 4.50. Control group was injected with the vehicle (1 ml $\times$ kg^{-1}, *ip.*) [59,60]. Rats were considered diabetic if their fasting blood glucose values were higher than 200 mg $\times$ dl^{-1} [61]. Rat blood glucose concentration after 72 h of STZ-injection was 423 ± 15 mg $\times$ dl^{-1}, while control animals showed normal glycemia of 120 ± 5 mg $\times$ dl^{-1}. After 28 days of STZ-injection, glucose values of both groups were tested and animals were sacrificed in a CO_2 atmosphere and hearts were removed. All the experimental procedures were performed using the whole heart.

It should be mentioned that a group of data included in this manuscript were obtained from the mitochondrial fraction of heart from animals included in our previous work [58].

However, in order to study other mitochondrial parameters or to increase the number of experimental replicates, new sets of animals were used using the same experimental protocol.

2.3. Heart mitochondrial isolation and mitochondrial membranes preparation

Heart mitochondrial fraction was obtained from tissue homogenates by differential centrifugation in a Sorvall RC5C centrifuge (Sorvall-Instruments-Du Pont, Model RC5S, Buckinghamshire, England). The hearts were isolated, washed, and minced in 5 ml of ice-cold medium containing 250 mM sucrose, 2 mM EGTA, 5 mM Tris-HCl, pH 7.40 (STE-1). The buffer was removed and a brief digestion was performed in STE medium supplemented with 0.5% (w/v) fatty acid-free BSA, 5 mM $MgCl_2$, 1 mM ATP and 2.5 U $\times$ ml^{-1} type XXIV bacterial proteinase, pH 7.40 (STE-2). After 4 min of incubation at 4 °C, the samples were homogenized in 1:10 STE-1 buffer with a glass-Teflon homogenizer and centrifuged at 8000*g* for 10 min. The pellet was resuspended in ice-cold STE-1 buffer and centrifuged at 700*g* for 10 min to remove nuclei and cell debris. The sediment was discarded and the supernatant was centrifuged at 8000*g* for 10 min to precipitate mitochondria. The pellet containing the mitochondrial fraction was washed twice and resuspended in STE-1 buffer. This suspension consisted of mitochondria able to carry out oxidative phosphorylation. Purity of isolated mitochondria was assessed by determining lactate dehydrogenase activity; only mitochondrial fractions with less than 10-15% of cytosolic lactate dehydrogenase activity were used. The whole procedure was carried out at 0-4 °C [30,62]. Protein concentration was determined with the Folin reagent [63] using bovine serum albumin as standard.

Mitochondrial membranes were obtained by three cycles of freezing and thawing of the mitochondrial preparation and homogenized by passage through a 25-gauge hypodermic needle [20].

2.4. Mitochondrial hydrogen peroxide production

Mitochondrial H_2O_2 production was followed fluorometrically at 365–450 nm (λ_{exc-em}) through the scopoletin–horseradish peroxidase (HRP) assay [64], using a Hitachi F-3010 fluorescence spectrophotometer. The reaction medium consisted of 230 mM mannitol, 70 mM sucrose, 20 mM Tris–HCl, pH 7.40, added with 0.5 μM Cu,Zn-SOD, 1 μM HRP, 1 μM scopoletin and coupled mitochondrial suspensions (0.1-0.3 mg protein× ml^{-1}). Mitochondrial H_2O_2 production rates, at 30 °C, were determined in state 4 using 6 mM malate and 6 mM glutamate as complex I substrates. A calibration curve was made using H_2O_2 (0.05-0.35 μM) as standard, previously titrated spectrophotometrically at 240 nm (ε = 43.6 M^{-1} cm^{-1}) to express the fluorescence changes as nmol $H_2O_2 \times min^{-1} \times$ mg $protein^{-1}$.

2.5. Mitochondrial nitric oxide production and NOS expression

2.5.1. NO production

Nitric oxide production by mitochondrial membranes was measured at 37 °C, following the oxidation of oxyhemoglobin (HbO_2) to methemoglobin at 577-591 nm (ε = 11.2 mM^{-1} cm^{-1}) using a Beckman DU 7400 diode array spectrophotometer [20,24,65]. The reaction medium consisted of 50 mM KH_2PO_4/K_2HPO_4, pH 7.40, 1 mM L-arginine, 1 mM $CaCl_2$, 100 μM NADPH, 10 μM dithiothreitol (DTT), 4 μM Cu,Zn-SOD, 0.1 μM catalase, 20 μM HbO_2 heme, and mitochondrial membranes suspensions (0.15-0.25 mg protein × ml^{-1}). In order to measure the "specific" NO production by mitochondria, only the HbO_2 oxidation inhibitable by 2 mM N^{ω}-monometil-L-arginine (L-NMMA) was considered. The absorbance changes were expressed as nmol NO × min^{-1} × mg $protein^{-1}$.

2.5.2. Mitochondrial NOS expression

To determine NOS expression in mitochondria, equal amounts of mitochondrial membranes (60-80 μg protein) were subjected to 7.5% sodium dodecyl sulfate–polyacrylamide gel electrophoresis (SDS-PAGE). Non-specific binding was blocked by incubation of the membranes with 5% non-fat dry milk in PBS for 1 h at room temperature.

Then, they were blotted into nitrocellulose films and probed with either 1:500 diluted rabbit polyclonal anti-neuronal NOS (H_{299}; cs-8309 Santa Cruz Biotechnology, Santa Cruz, CA) or 1:500 diluted goat polyclonal anti-VDAC-1 (D-16: sc-32063, Santa Cruz Biotechnology, Santa Cruz, CA) antibodies. The nitrocellulose membranes were subsequently incubated with a secondary goat anti-rabbit IgG antibody (GAR:170-5046; Bio-Rad, CA) or a mouse anti-goat antibody (IgG-HRP, sc: 2354, Santa Cruz Biotechnology, Santa Cruz, CA) (dilution 1:5000), respectively. The secondary antibodies were conjugated with horseradish peroxidase and were revealed by chemiluminiscence with ECL reagent. Densitometric analysis of the bands was performed by Image 1.62 software (Wayne Rasband, NIH, Bethesda, MD, USA) and data were expressed as relative to VDAC-1 expression (loading control) [66].

2.6. Mitochondrial ATP production

The assay is based on the chemiluminescent detection using the luciferin-luciferase reaction [67]. The ATP production was measured in coupled mitochondria (0.15 - 0.50 mg protein × ml^{-1}) in a reaction medium containing 120 mM KCl, 20 mM Tris-HCl, 1.6 mM EDTA, 0.08% BSA, 8 mM K_2HPO_4/KH_2PO_4, 0.08 mM $MgCl_2$, pH 7.40 (Buffer A) and 40 μM D-luciferin, 20 μg ×ml^{-1} luciferase and 0.50 mM Tris-Acetate pH 7.75 (Buffer B), at 30 °C. ATP production was triggered by the addition of 3 mM malate and 1.25 mM glutamate or 8 mM succinate, 0.1 mM ADP and 0.15 mM di-(adenosine) pentaphosphate, to the reaction medium. Chemioluminescence emission was followed as a function of time in a LabSystem Luminoskan EL microplate reader (LabSystem, MN, US). As negative control, 2 μM oligomycin were added to inhibit the F_o subunit of the F_oF_1-ATP synthase. A calibration curve was performed using ATP (10 - 100 nmol) as standard. ATP production rate was expressed as nmol ATP × min^{-1} × mg $protein^{-1}$ [68].

2.7. Mitochondrial membrane potential

Mitochondrial membrane potential was measured by flow cytometry [69] using a Partec PAS-III flow cytometer (Partec GmbH, Münster, Germany) equipped with a 488 nm argon laser.

In order to select the mitochondrial population, 10-N-nonyl acridine orange (NAO) was used. This probe selectively stains mitochondria through its ability to bind to the cardiolipin located in the inner mitochondrial membrane [70]. Freshly isolated mitochondria (0.5 mg protein × ml^{-1}) were incubated in the dark with 7.5 μM NAO, for 20 min at 37 °C. Samples were gated based on light scattering properties, and 30 000 events per sample within this gate (R1) were collected, excluding cellular debris and damaged mitochondria.

To estimate the inner mitochondrial membrane potential, freshly isolated mitochondria (0.5 mg protein × ml^{-1}) suspended in a reaction medium containing 0.20 M mannitol, 0.07 M sucrose, 5.5 mM Hepes and 100 mM KH_2PO_4/K_2HPO_4, pH 7.40 (MSHP) were incubated in dark with the potentiometric cationic probe 3,3´-dihexyloxacarbocyanine iodide ($DiOC_6$) (90 nM), for 20 min at 37 °C. The changes in membrane potential after the addition to the reaction medium of 2 mM malate and 5 mM glutamate or 8 mM succinate, to establish state 4, and the supplementation with 1 mM ADP, to induce state 3, were analyzed through the $DiOC_6$ signal in the FL-1 channel with Cyflogic software (CyFlo Ltd, Turku, Finland). The total depolarization induced by 40 μM m-CCCP was used as a positive control [71].

2.8. Mitochondrial biogenesis markers

2.8.1. Mitochondrial mass

Because the cytochrome oxidase enzyme is solely located in mitochondrial membranes, the content of heart mitochondria (*i.e.* mitochondrial mass) in diabetic and control animals was estimated from the ratios of cytochrome oxidase activities in heart homogenates and in the mitochondrial fraction [72–74]. Thus, complex IV activity was determined in homogenates (0.005-0.010 mg protein × ml^{-1}) and in mitochondrial fraction

(0.003-0.010 mg protein × ml^{-1}) suspended in 100 mM KH_2PO_4/K_2HPO_4 pH 7.40 and supplemented with 50 μM cytochrome c^{2+} [75,76]. The rate of cytochrome c^{2+} oxidation by complex IV was calculated as the pseudo-first-order reaction constant (k´) and expressed as min^{-1}×mg $protein^{-1}$ or min^{-1} × g $tissue^{-1}$ depending on mitochondrial membranes or homogenates were used, respectively. The ratio between the activity measured in total homogenates (k´ × g $tissue^{-1}$) and the activity determined in mitochondrial membranes (k´ × mg $protein^{-1}$) yields the mitochondrial mass per gram of tissue. Reduced cytochrome *c* was freshly prepared by reduction of cytochrome c^{3+} with $Na_2S_2O_4$ followed by Sephadex G-25 chromatography [58].

2.8.2. Mitochondrial electron microscopy and Stereological Analysis

The study of the mitochondrial ultrastructure was performed by transmission electron microscopy (TEM) in 1 mm^3 tissue sample. Hearts obtained from control and diabetic animals were washed with 100 mM K_2HPO_4/KH_2PO_4, pH 7.40 and then cut in cubes of 1 mm^3 by a scalpel. Tissue samples were fixed with 2.5% glutaraldehyde in 100 mM K_2HPO_4/KH_2PO_4, pH 7.40 during 1 h at 0 °C and post-fixed in 1% (v/v) osmium tetroxide in 100 mM K_2HPO_4/KH_2PO_4 for 90 min at 0 °C. Samples were incubated with 5% uranyl acetate for 2 h at 0 °C, dehydrated by successive passages in solutions with increasing concentrations of ethanol and incubated with propylene oxide for 15 min. Samples were embedded in Durcupan resin (Fluka AG, ChemischeFabrik, Buchs SG, Switzerland) for 72 h at 60 °C. Ultrathin sections (50 nm) were cut using an ultramicrotome (Reichert Jung Utracut E.) and observed with a Zeiss EM 109 transmission electron microscope (Oberkochen, Germany). Representative digital images were captured using a CCD GATAN ES1000W camera (California, USA). Random sections were selected for analysis by an electron microscopy technician blinded to the treatments.

From the images obtained, a stereological analysis was performed. For this, samples from 3 control and 4 diabetic animals were used and between 12 and 25 photos were

obtained from each sample. We quantified the number of mitochondria per area, the mean area occupied by each mitochondrion in the cardiac tissue and the mitochondrial volume density, using the Image Pro-Plus 6.0 Software (Media Cybernetics, Inc.Rockville, USA). From these data we performed a stereological analysis of mitochondria, *i.e.* the spatial interpretation of the plane sections.

The *mitochondrial volume density (V_{mi})*, which represents the volume of cytosol occupied by mitochondria, was determined using the *"point counting grids"* methodology [77] and expressed as a percentage. The *mitochondrial numerical density (N_{mi})*, which represents the number of mitochondria per unit volume, was calculated using the following expression:

$$N_{mi} = \frac{1}{\beta} \times \frac{N_a^{3/2}}{V_{mi}^{1/2}} \times K$$

where N_a is the number of mitochondria per each μm^2, V_{mi} is the mitochondrial volume density, β is a coefficient which depends on the shape of the organelle, and K is a factor dependent on the size distribution of the organelle (β = 2.25 and K = 1 for mitochondria). The number of mitochondria was counted in an area of 112 μm^2 using an amplification of 12 000X. N_{mi} was expressed as a percentage.

2.8.3. PGC-1α expression

In the case of the expression of the transcription factor peroxisome proliferator-activated receptor-gamma coactivator (PGC-1α), equal amounts of heart total homogenate (100 μg protein) were subjected to 10% SDS-PAGE. After the same procedures described in section 2.5.2 they were blotted into nitrocellulose films and probed with 1:500 diluted goat polyclonal antibodies against PGC-1α (K-15: sc-5816; Santa Cruz Biotechnology, Santa Cruz, CA) with a secondary mouse anti-goat antibody diluted 1:5000. The secondary antibodies were conjugated with horseradish peroxidase and were revealed by chemiluminiscence with ECL reagent. β-actin expression was used as a loading control (mouse monoclonal anti β-actin diluted 1:500; C4: sc-47778; Santa Cruz Biotechnology,

Santa Cruz, CA; with a secondary rabbit anti-mouse antibody diluted 1:5000). Densitometric analysis of the bands was performed and data were expressed as relative to β-actin expression.

2.9. Statistics

Results included in tables and figures are expressed as means ± SEM and represent replicated measurements on at least three to seven independent experiments. Student's t-test was used to analyze the significance of differences between Control and Diabetic groups. Values of $p<0.05$ and $p<0.01$ were considered statistically significant and highly significant, respectively. Statistical analysis was done using GraphPadnstat 4 (GraphPad Software, La Jolla, CA, USA).

3. RESULTS

3.1. Mitochondrial H_2O_2 and NO production rates and mtNOS expression

The H_2O_2 production rate of heart mitochondria from diabetic animals sustained by malate-glutamate was 2-fold the H_2O_2 generation detected in control mitochondria (Fig. 1A).

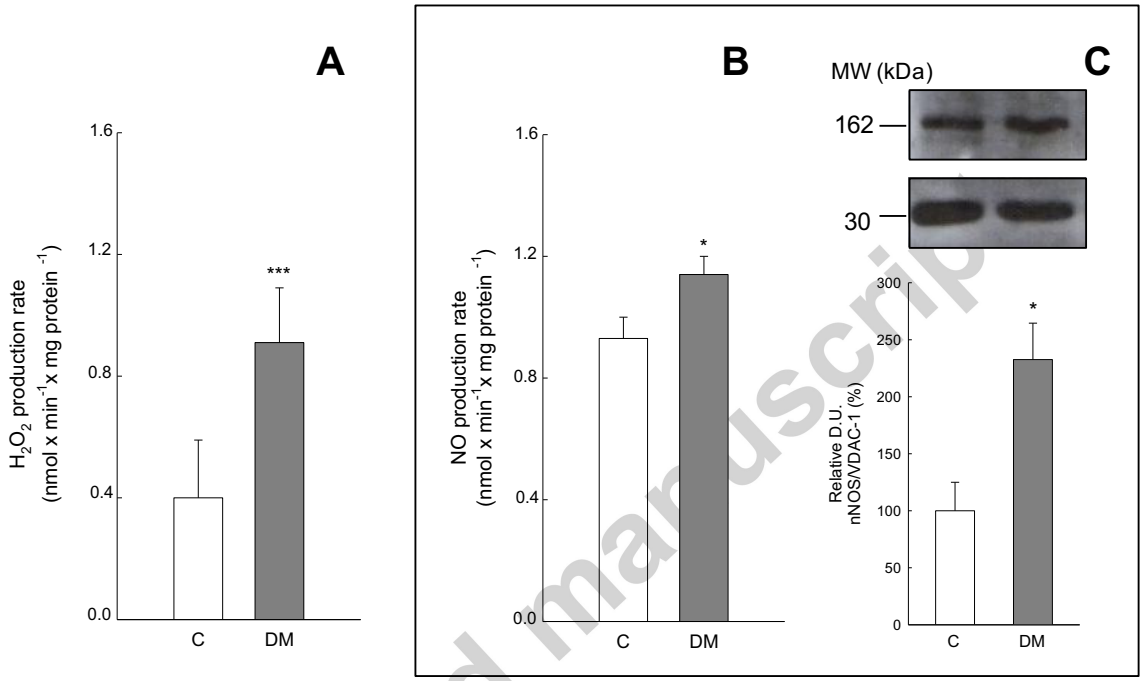

Fig 1. Heart mitochondrial H_2O_2 **(A)** and NO **(B)** production rates from control (white bars) and diabetic rats (grey bars). **(C)** NOS expression in heart mitochondrial fraction. Western blot analysis of heart mitochondrial membranes using anti-nNOS H_{299} antibodies (MW: 162 kDa, upper panel) and VDAC-1 antibodies (MW: 30 kDa, lower panel) as loading control (Santa Cruz Biotech.). Plot showing the densitometric units ratio between nNOS and VDAC 1, expressed as the percentage relative to control. *p< 0.05; ***p < 0.005, significantly different respect to control group (Student´s t test). Control (C, n = 4); Diabetes (DM, n = 6).

The NO production rate by heart mitochondrial membranes, *i.e.* the mtNOS activity, was significantly increased by 23% in the diabetic rats in comparison with control animals (Fig. 1B). The expression of NOS in the heart mitochondrial fraction using anti-nNOS

antibodies was analyzed. As Fig. 1C shows, the mtNOS expression in heart from diabetic animals was about 132% higher than the NOS expression detected in control group, in accordance with the enhancement in mitochondrial NO production (Fig. 1B) observed in the animals injected with STZ.

3.2. Mitochondrial membrane potential and ATP production rate

Mitochondrial membrane potential, *i.e.* the electrical component of the electrochemical potential generated by the H^+ pumping to the intermembrane space, was measured using flow cytometry (Fig. 2). Mitochondria were selected from background based on its light scattering properties (SSC: *Side Scattervs.* FSC: *Forward Scatter)* and events within gate R1, ~30 000 events, were chosen for analysis. Between 60-70% of the events within R1 gate were NAO-positive (R2) compared with the auto-fluorescence signal corresponding to unstained control samples.As it is shown in the overlaid histograms (Fig. 2A), STZ treatment induced a slightly decrease in FL1 $DiOC_6$ signal when mitochondria were respiring in state 3 both using malate-glutamate and succinate as substrates, in comparison with the control group. This phenomenon is observed as a shift to the left in the histograms, *i.e.* a lower fluorescence intensity of the $DiOC_6$ probe, corresponding to heart mitochondria from diabetic animals. In contrast, no differences between groups were observed in state 4 mitochondria, neither supported by malate-glutamate nor succinate. As expected, a strong depolarization was induced by the addition of m-CCCP to the reaction medium in both groups *(data not shown)*.

The quantification of $DiOC_6$ fluorescence intensity of gated (R1) histograms corresponding to the state 3 mitochondrial membrane potential of heart from diabetic and control animals, and the total depolarization after the addition of the uncoupler m-CCCP are included in Fig. 2B. Thus, a significantly lower percentage of visible events in the R1 gate (22%) has been observed when mitochondria from diabetic animals are respiring in state 3 using malate-glutamate. Although the shift to the left was also observed when mitochondria were respiring in state 3 using succinate as substrate, this change was not statically

significant, suggesting a partial depolarization of mitochondria mainly when the electrons entered through complex I.

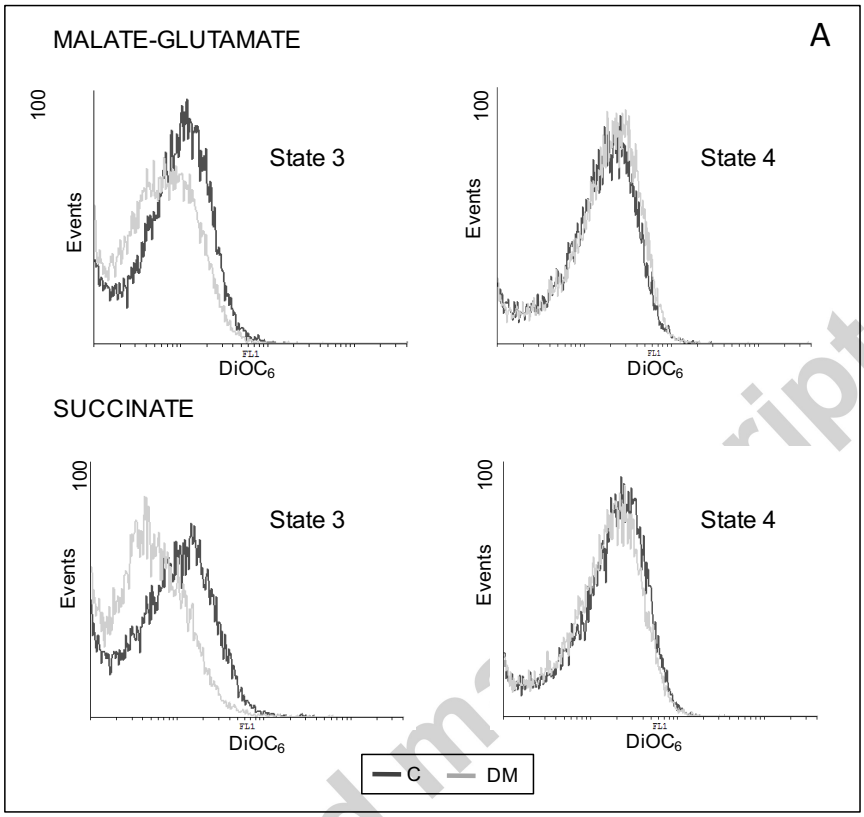

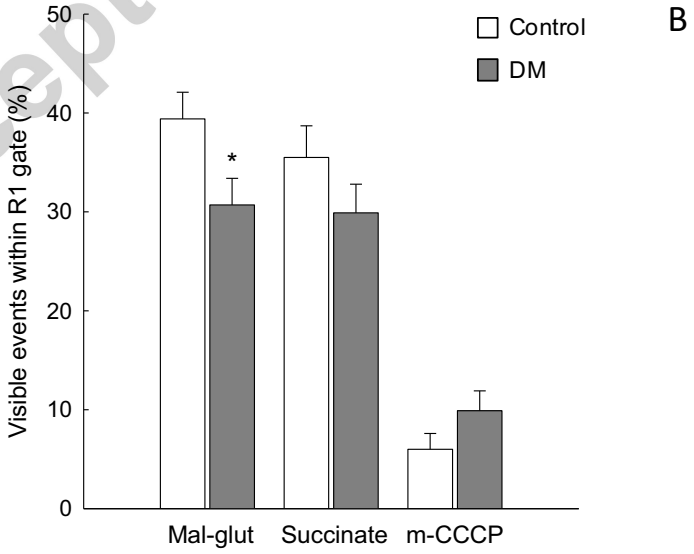

Fig 2. Heart mitochondrial membrane potential. **(A)** Overlaid histograms of gated (R1) mitochondrial events vs. DiOC6 fluorescence intensity. State 4 and state 3 membrane potentials were evaluated in coupled mitochondria of control (dark grey line) or diabetes animals (grey line) using malate-glutamate or succinate as substrates. **(B)** DiOC6 fluorescence intensity quantification of gated (R1) histograms corresponding to mitochondria from control (white bars) or diabetic animals (dark grey bars) respiring in state 3. Mitochondrial depolarization induced by m-CCCP was used as positive control. Results are expressed as the percentage of visible events within R1.

* $p < 0.05$, significantly different respect to control group (Student´s t test). Control (C, n = 4), Diabetes (DM, n = 5).

Considering that the electrochemical H^+ gradient across the inner mitochondrial membrane is the driving force for ATP synthesis, ATP production by heart mitochondria from control and diabetic animals was measured both using complex I and complex II substrates. Fig. 3 shows that ATP production rate was 44% or 37% lower in heart mitochondria from diabetic animals than from control rats, when malate-glutamate or succinate were used, respectively. These results indicate energy production impairment, in accordance with the partial depolarization of heart mitochondria from diabetic animals.

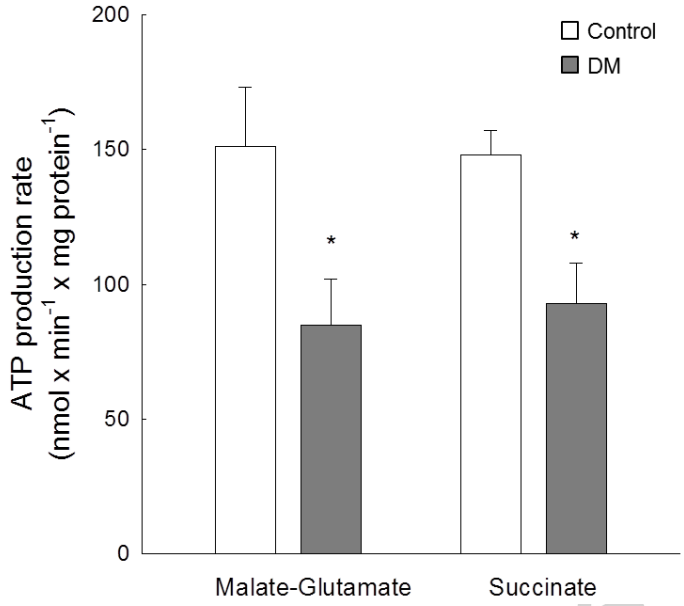

Fig 3. ATP production rate by heart mitochondria from control (white bars) and diabetic rats (grey bars), using malate-glutamate or succinate as substrates. * $p < 0.05$, significantly different respect to control group (Student´s t test). Control (C, n = 4), Diabetes (DM, n = 6)

3.3. Mitochondrial biogenesis

3.3.1. Mitochondrial mass

Mitochondrial mass, expressed as mg mitochondrial protein per grams of tissue, was determined by the ratio of complex IV activity measured in total homogenate, expressed as $min^{-1} \times g\ tissue^{-1}$, and the activity in the mitochondrial fraction, expressed as $min^{-1} \times mg\ protein^{-1}$. The cytochrome oxidase activity measured in heart homogenate was not statistically different between groups (Fig. 4A). On the contrary, complex IV activity measured in the mitochondrial fraction was 22% lower in diabetic animals than in control rats (Fig. 4B). As a consequence, the proportion of mitochondrial mass per tissue mass was 47% higher in diabetic hearts than in control hearts (Fig. 4C), suggesting a mitochondrial

biogenesis process with *de novo* synthesis of new mitochondrial proteins in the STZ-treated animals triggered in response to the hyperglycemic status.

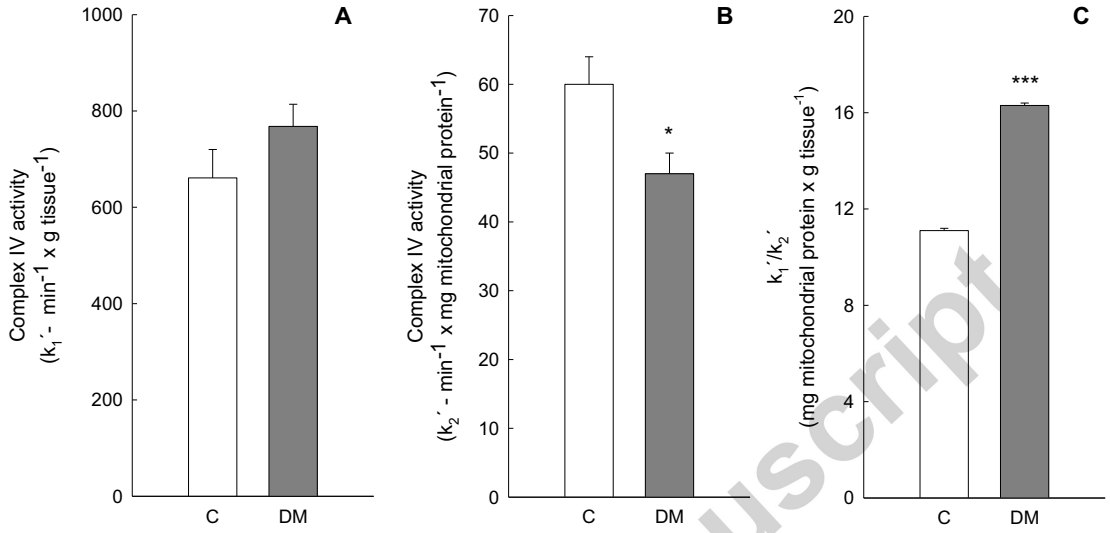

Fig 4. Cytochrome oxidase (complex IV) activity as an index of mitochondrial biogenesis. **(A)** Complex IV activity in heart homogenates ($k_1´$). **(B)** Complex IV activity in heart mitochondrial fraction ($k_2´$). **(C)** $k_1´/ k_2´$ ratio as an index of mitochondrial mass, expressed as mg mitochondrial protein per gram of tissue. *$p < 0.05$; *** $p < 0.005$, significantly different respect to control group (Student´s t test). Control (C, n = 5), Diabetes (DM, n = 7).

3.3.2. Electron microscopy and stereological analysis of cardiac tissue

Electron microscope images form diabetic cardiac tissue show a higher number of mitochondria with variable shapes respect to control heart, disorganized and damaged with structural alterations such as *swelling*, loss of cristae and external membrane (Fig. 5).

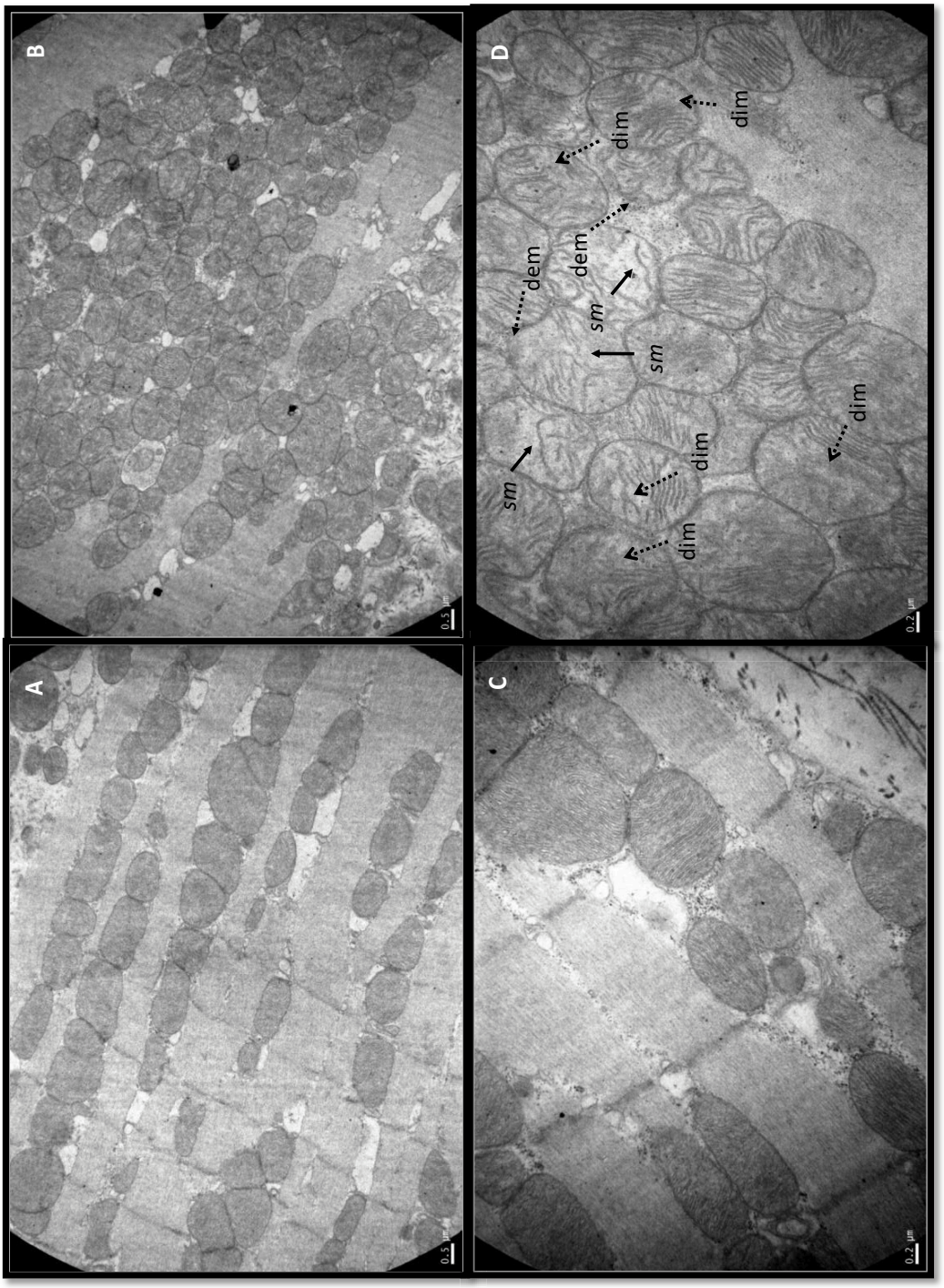

Fig 5. Electron transmission microscope microphotographs of cardiac tissue of a control (**A and C**) and a diabetic (**B and D**) rats. Figure **B** shows a higher number of mitochondria in cardiac tissue of diabetic animals, accompanied by mitochondrial disorganization in the muscle fiber respect to control tissue (**A**). Additionally, in Figure **B** it can be observed a variability of mitochondrial shapes and sizes,

in cardiac tissue from diabetic rats. Figure **D** shows cardiac mitochondria from diabetic animals in a higher augment, with the presence of mitochondrial alterations; *e.g.* disruption of the internal and external membrane (*dim* and *dem*, dotted arrows) and mitochondrial *swelling* (*ms*, full arrows). Scale bars: A and B, 0.5 μm; C and D, 0.2 μm.

The performed stereological analysis of heart mitochondria, included: the fraction of cytosolic volume occupied by mitochondria, *i.e.* the mitochondrial volume density (V_{mi}), the number of mitochondria per area (N_a), and the mitochondrial numerical density (N_{mi}).

To estimate V_{mi}, approximately 40 microphotographs of cardiac tissue from 3 control rats and 60 microphotographs from 4 diabetic rats were analyzed. Thus, the V_{mi} of cardiac tissue from diabetic animals was 30% higher than the one detected in control cardiac tissue (Table 1). Nonetheless, the mean area of each mitochondrion, expressed in μm^2, was reduced by 23% in heart of diabetic animals respect to the mean area in control tissues. Hence, as each mitochondrion is smaller in diabetic than in control cardiac tissue, the increase in V_{mi} is due to a higher number of mitochondria per tissue mass. This result was confirmed with the counting of mitochondria in a microscope field area at 12 000X augment (112 μm^2) and referred to 1 μm^2, *i.e.* the number of mitochondria per unit area (N_a). This value in the cardiac tissue from diabetic animals (0.67 ± 0.02 mitochondria × μm^{-2}) was 53% higher than the one in control tissues (0.44 ± 0.06 mitochondria × μm^{-2}).

Mitochondrial numerical density (N_{mi}), which expresses the number of mitochondria counted per unit volume, was calculated using the formula described by Weibel et al. [78]. As shown in Table 1, N_{mi} was enhanced by 66% in the cardiac tissue from diabetic animals respect to control tissue. Therefore, this result agrees with the increment observed in the mitochondrial mass estimated from complex IV activity (Fig. 4C), and suggests the presence of an active mitochondrial biogenesis process.

Table 1. Stereological analysis of cardiac tissue mitochondria from control and diabetic animals

Stereological parameters	Control	Diabetes
Mitochondrial volume density (V_{mi})	0.30 ± 0.01	0.39 ± 0.01***
Mitochondrial volume density (V_{mi}; %)	30	39***
Mitochondrial mean area (μm^2)	0.70 ± 0.06	0.54 ± 0.06
N° mitochondria per area (mitochondria$\times\mu m^{-2}$)	0.44 ± 0.06	0.67 ± 0.02***
Mitochondrial numerical density (N_{mi}; %)	100	166*

*p < 0.05; ***p < 0.005 significantly different respect to control group (Student´s t test).
Control (n = 3), Diabetes (n = 4). 12 to 25 photos were taken from each sample.

3.3.3. PGC-1α as biogenesis marker

The expression of the transcription factor PCG-1α, which is involved in the signaling cascade that carry out to mitochondrial biogenesis, was analyzed in homogenates obtained from the heart of control and diabetic animals (Fig. 6A). Figure 6B illustrate the densitometric units relative to β-actin, this latter used as a loading control. An enhancement in PGC-1α expression of 76% was observed (Fig. 6B) at the end of the treatment, in heart homogenates from diabetic animals with respect to the levels expressed in control animals, in agreement with the higher mitochondrial mass per tissue mass estimated and showed above (Figs. 4, Table 1).

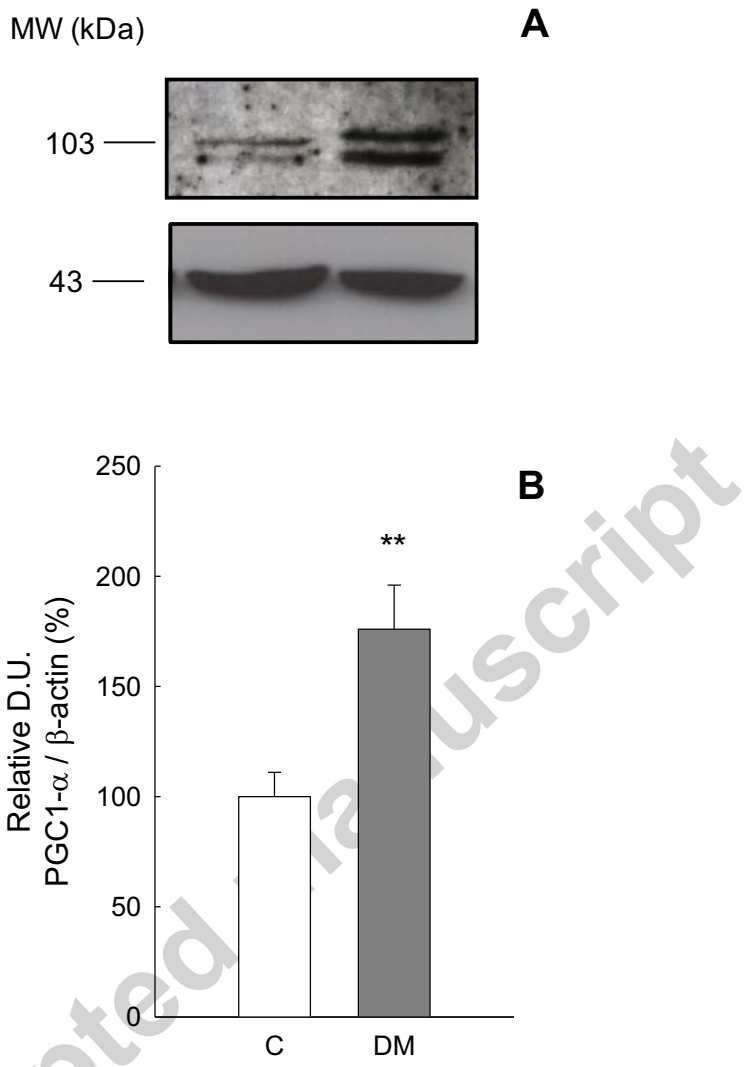

Fig 6. PGC-1α expression in heart homogenates. **(A)** Western blot using anti-PGC-1α antibodies (MW: 103 kDa, upper panel) and anti-β actin antibodies (MW: 43 kDa, lower panel) as loading control (Santa Cruz Biotech.). **(B)** Plot showing the densitometric units ratio between PGC-1α and β-actin in heart homogenate from control and diabetic animals, expressed as the percentage relative to control (100%).**$p < 0.01$, significantly different respect to control group (Student´s t test). Control (C, n = 3), Diabetes (DM, n = 4).

4. DISCUSSION

The results presented in this work provide evidence that mitochondrial biogenesis is enhanced in hearts of STZ-induced diabetic rats. Changes in the steady-state concentrations of the mitochondrial molecules H_2O_2 and NO and in the ATP level could be involved in the signaling pathways that lead to *the novo* synthesis of mitochondria.

It is known that organs that demand large amounts of energy, such as heart, are particularly susceptible to an energy crisis and concomitantly to cell death. Mitochondria generate 95% of cellular ATP by oxidative phosphorylation, supplying the cardiomyocytes with the energy needed to maintain normal contractile function. Mitochondrial function depends on the electrochemical gradient of H^+ that is established through the inner mitochondrial membrane, carried out by the activity of the respiratory chain complexes, being this gradient the driving force for ATP synthesis. In this work, a partial depolarization of the inner mitochondrial membrane of heart of diabetic rats was observed when mitochondria were respiring in state 3 (Fig. 2), mainly when the electrons entered through Complex I. Furthermore, ATP production rate was about 40% lower in heart mitochondria from diabetic than from control animals (Fig. 3).These data are in agreement with the lower mitochondrial complexes activities and ADP/O ratio previously observed [58] in hearts of diabetic respect to control animals. Therefore, a mitochondrial energetic state impairment occurs in heart of diabetic animals which could lead to a reduced supply of energy to the rest of the cell.

Mitochondria not only generate ATP that supports the energy demands of cardiomyocytes but also produce second messengers, such as H_2O_2, NO and $ONOO^-$, implicated in the modulation of redox sensitive signaling pathways and in the regulation of NAD^+/NADH homeostasis, influencing the activation of the cofactor PGC-1α [17]. At present, H_2O_2 is considered as the major redox metabolite operative in redox sensing, signaling and redox regulation [45]. The generation of H_2O_2 reports the mitochondrial energy charge to the cytosol and is implicated in the regulation of the cellular redox status, thus transducing redox signals into a wide variety of responses, such as proliferation, differentiation, and cellular

death pathways. The role of H_2O_2 in redox signaling depends on its steady-state concentration and its suborganellar distribution [45]. Under our experimental conditions, an increase in H_2O_2 production rate was observed only when mitochondria were supplemented with complex I substrates (Fig. 1A), suggesting structural modifications of complex I proteins in heart of diabetic rats [24,34,35]. Additionally, an increase not only in NO production (Fig. 1B) but also in mtNOS expression (Fig. 1C) were observed in the heart of diabetic animals, indicating that NO could participate as a signaling molecule, leading to mitochondrial biogenesis [51,52]. This compensatory mechanism might be an adaptive response to replace damaged and dysfunctional mitochondria and to restore the bioenergetics function that is altered in hearts of diabetic animals. This process was evaluated focusing on different approaches: a) *de novo* synthesis of mitochondrial proteins, b) stereological analysis of heart mitochondria, and c) expression of the transcription factor PGC-1α. The data obtained showed that mitochondrial mass per tissue mass was 47% higher in diabetic than in control cardiomyocytes (Fig. 4C), indicating the activation of the biogenesis process. This result was confirmed by the stereological analysis of cardiac tissue microphotographs (Figs. 5 and Table 1), in which a 30% increment in the cellular volume occupied by mitochondria was observed in diabetic hearts, with a smaller mitochondrial size (23%) than in control hearts. Thus, the higher V_{mi} observed in hearts from diabetic animals was due to a higher number of mitochondria per unit area (52%). Additionally, the number of mitochondria per unit volume (N_{mi}) showed an increment of 66% in agreement with the enhancement in mitochondrial mass. Furthermore, an increase (76%) in the expression of the transcription factor PGC-1α was observed (Fig. 6B). To note, this is one of the main regulators of mitochondrial biogenesis in cardiac muscle, skeletal muscle and adipose tissue [79–81] and its expression is regulated by oxygen or nitrogen reactive species [82]. The expression of this transcription factor has been positively associated with glucose capture and oxidation and with a higher expression of the glucose transporter GLUT-4 [83]. Figure 7 shows that the enhancement in H_2O_2 and NO production rates are accompanied to an increase in the number of

mitochondria per unit area, in heart of diabetic respect to control animals. Thus, the overall results presented in this work along with the linear correlations observed in Fig. 7 support the idea that mitochondrial biogenesis is activated in diabetic hearts, and both NO and H_2O_2 could act as signaling molecules involved in the process that leads to *the novo* synthesis of mitochondria.

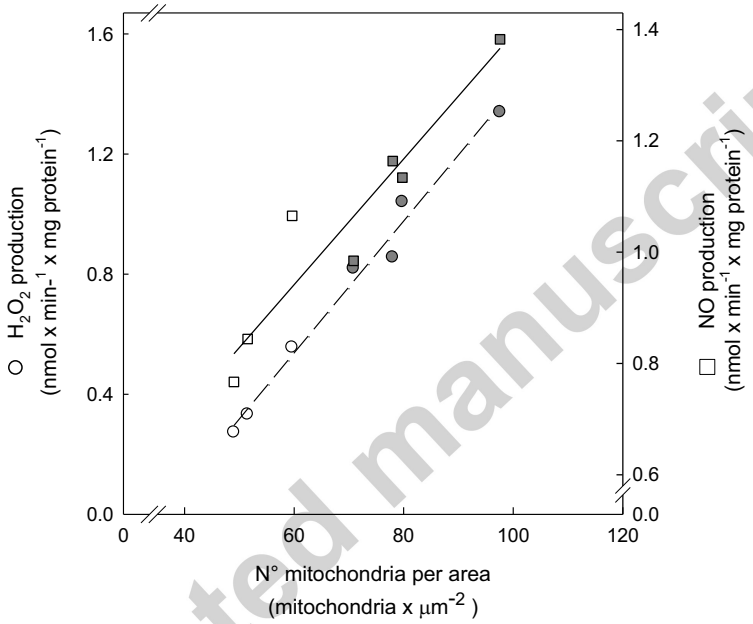

Fig 7. Linear correlation between the number of mitochondria per unit area, as an index of mitochondrial biogenesis, and H_2O_2 (circles, $r^2 = 0.983$) or NO (squares, $r^2 = 0.896$) production rates, in heart of diabetic (grey) respect to control (white) animals.

Taking into account the experimental values of H_2O_2 and NO production rates and the active Mn-SOD concentration in the mitochondrial matrix (control 17 μM and diabetic 8.5 μM; [58]), NO and $O_2^{\bullet-}$ steady-state concentrations can be calculated [35,84] *(Details of the calculation procedure were included in the supplementary material)*. Table 2 shows that $[NO]_{ss}$ is enhanced by 20% in heart mitochondria from diabetic animals respect to controls, in accordance with the increment observed in NO production rate and the enhancement in

mtNOS expression (Fig. 1). Additionally, the $[O_2^{\bullet-}]_{ss}$ calculated was 4 times higher in diabetic than control animals. Thus, the increase in H_2O_2 production rate measured in mitochondria from diabetic animals was due to a higher $O_2^{\bullet-}$ steady-state concentration, even in the presence of Mn-SOD activity reduction.

Table 2. NO and $O_2^{\bullet-}$ steady-state concentrations and $ONOO^-$ formation in heart mitochondria from control and diabetic animals

Group	$[NO]_{ss}$	$[O_2^{\bullet-}]_{ss}$	$d[ONOO^-]/dt$
	(10^{-9} M)	(10^{-11} M)	(nM s^{-1})
Control	9.40	4.71	8.40
Diabetes	11.4	21.3	46.0

In addition, the rate of $ONOO^-$ formation can be calculated by considering the steady-state concentrations of NO and $O_2^{\bullet-}$ in the mitochondrial matrix and the second-order rate constant k = 1.9×10^{10} M^{-1} s^{-1} [85]. Table 2 shows that $ONOO^-$ production rate was 5 times higher in heart mitochondria from diabetic than from control rats. Whereas in physiological situations only 15% of the $O_2^{\bullet-}$ generated in the mitochondria is metabolized through the reaction with NO to form $ONOO^-$, in situations in which Mn-SOD activity is reduced and NO generation is enhanced, the catabolic pathway of $O_2^{\bullet-}$ that yields $ONOO^-$ could be exacerbated. Moreover, $ONOO^-$ generation rate seems to be mainly controlled by $O_2^{\bullet-}$ steady-state concentration rather than by NO steady-state concentration. Furthermore, these results agree with the increase in protein tyrosine nitration (~60%) observed in heart mitochondria obtained from diabetic animals [58].

Hence, the results presented in this work suggest that in order to increase the number of mitochondria and to supply the energetic dysfunction that occurs as a consequence of hyperglycemia, mitochondrial biogenesis is triggered in the heart of diabetic animals. Nisoli and colleagues [2] showed that the stimulation of mitochondrial biogenesis by an NO donor

in cell lines generates new and functional mitochondria. Nevertheless, in this work mitochondrial biogenesis was not accompanied with the recovery of the mitochondrial function and energy bioavailability for the tissue. Mitochondria from diabetic animals showed the presence of structural alterations (mitochondrial *swelling*, loss of cristae and disruption of inner and outer membranes) along with changes in mitochondrial bioenergetics, *e.g.* a partial depolarization of the inner mitochondrial membrane and a lower ATP production rate. Concomitantly with these observations, previous results of our group [58] with the same experimental protocol, showed a heart mitochondrial dysfunction characterized by reduction in mitochondrial respiration, in the activity of respiratory chain complexes and in the efficiency of oxidative phosphorylation, leading to alterations in cardiac bioenergetics and to a cardiac compromise against a work overload. It is worth noting that the biogenesis process triggered *in vivo* in an organism, in physiopathological conditions, not necessarily results in the generation of functionally active mitochondria. Bugger and Abel [86] had reported an increase in mitochondrial biogenesis in cardiomyocytes from diabetic mice, without an improvement of the mitochondrial function. Studies in transgenic mice that over express PCG-1α, show that although the biogenesis process is activated, the mitochondrial function is not recovered in the same magnitude [87].

To conclude, changes in the steady-state concentrations of H_2O_2 and NO and an imbalance between cellular energy demand and mitochondrial energy transduction could lead to mitochondrial biogenesis. Because of the sustained hyperglycemia that occurs in our experimental model, this compensatory mechanism triggered to restore the mitochondrial and tissue normal activities did not lead to competent mitochondria capable of supplying the energetic demands.

ACKNOWLEDGMENTS

This work was supported by research grants from the University of Buenos Aires (UBACyT 200-201-101-00140, 200-201-301-00731), Agencia Nacional de Promoción Científica y Tecnológica (ANPCyT, PICT 2014-0964), and Consejo Nacional de Investigaciones Científicas y Técnicas (CONICET; PIP 112-201-101-00444).

REFERENCES

[1] L. Moran, J. Gutteridge, G. Quinlan, Thiols in cellular redox signalling and control, Curr Med Chem. 8 (2001) 763–772. https://www.ncbi.nlm.nih.gov/pubmed/?term=Moran+LK%2C+Gutteridge+JM%2C+and+Quinlan+GJ.+Thiols+in+cellular+redox+signalling+and+control.+Curr+Med+Chem+8%3A+763%E2%80%93+772%2C+2001.

[2] E. Nisoli, E. Clementi, S. Moncada, M.O. Carruba, Mitochondrial biogenesis as a cellular signaling framework, Biochemical Pharmacology. 67 (2004) 1–15. doi:10.1016/j.bcp.2003.10.015.

[3] A. Boveris, B. Chance, The mitochondrial generation of hydrogen peroxide. General properties and effect of hyperbaric oxygen, Biochem J. 134 (1973) 707–716. http://www.ncbi.nlm.nih.gov/entrez/query.fcgi?cmd=Retrieve&db=PubMed&dopt=Citation&list_uids=4749271.

[4] A. Boveris, E. Cadenas, Mitochondrial production of superoxide anions and its relationship to the antimycin insensitive respiration, FEBS Lett. 54 (1975) 311–314. http://www.ncbi.nlm.nih.gov/entrez/query.fcgi?cmd=Retrieve&db=PubMed&dopt=Citation&list_uids=236930.

[5] J.F. Turrens, A. Boveris, Generation of superoxide anion by the NADH dehydrogenase of bovine heart mitochondria, Biochem J. 191 (1980) 421–427. http://www.ncbi.nlm.nih.gov/entrez/query.fcgi?cmd=Retrieve&db=PubMed&dopt=Citation&list_uids=6263247.

[6] A. Boveris, E. Cadenas, A.O. Stoppani, Role of ubiquinone in the mitochondrial generation of hydrogen peroxide, Biochem J. 156 (1976) 435–444. http://www.ncbi.nlm.nih.gov/entrez/query.fcgi?cmd=Retrieve&db=PubMed&dopt=Citation&list_uids=182149.

[7] E. Cadenas, A. Boveris, C.I. Ragan, A.O. Stoppani, Production of superoxide radicals and hydrogen peroxide by NADH-ubiquinone reductase and ubiquinol-cytochrome c reductase from beef-heart mitochondria, Arch Biochem Biophys. 180 (1977) 248–257. http://www.ncbi.nlm.nih.gov/entrez/query.fcgi?cmd=Retrieve&db=PubMed&dopt=Citation&list_uids=195520.

[8] B. Chance, H. Sies, a Boveris, Hydroperoxide metabolism in mammalian organs., Physiological Reviews. 59 (1979) 527–605.

[9] P. Ghafourifar, C. Richter, Nitric oxide synthase activity in mitochondria, FEBS Lett. 418 (1997) 291–296. http://www.ncbi.nlm.nih.gov/entrez/query.fcgi?cmd=Retrieve&db=PubMed&dopt=Citation&list_uids=9428730.

[10] C. Giulivi, J.J. Poderoso, A. Boveris, Production of nitric oxide by mitochondria, J Biol Chem. 273 (1998) 11038–11043. http://www.ncbi.nlm.nih.gov/entrez/query.fcgi?cmd=Retrieve&db=PubMed&dopt=Citation&list_uids=9556586.

[11] A. Tatoyan, C. Giulivi, Purification and characterization of a nitric-oxide synthase from rat liver mitochondria, J Biol Chem. 273 (1998) 11044–11048. http://www.ncbi.nlm.nih.gov/entrez/query.fcgi?cmd=Retrieve&db=PubMed&dopt=Citation&list_uids=9556587.

[12] T. Zaobornyj, L. Valdez, Heart mitochondrial nitric oxide synthase: a strategic enzyme in the regulation of cellular bioenergetics., Vitamins and Hormones. 96 (2014) 29–58. doi:10.1016/B978-0-12-800254-4.00003-9.

[13] T. Zaobornyj, D.E. Iglesias, S.S. Bombicino, I.A. Rukavina Mikusic, L.B. Valdez, Biochemistry and physiology of heart mitochondrial nitric oxide synthase, in: R.J. Gelpi, A. Boveris, J. Poderoso (Eds.), Biochemistry of Oxidative Stress Physiopathology and Clinical Aspects, Springer Nature, Switzerland, 2016: pp. 37–48. doi:10.1007/978-3-319-45865-6.

[14] S.L. Elfering, T.M. Sarkela, C. Giulivi, Biochemistry of mitochondrial nitric-oxide synthase, J Biol Chem. 277 (2002) 38079–38086. http://www.ncbi.nlm.nih.gov/entrez/query.fcgi?cmd=Retrieve&db=PubMed&dopt=Citation&list_uids=12154090.

[15] A. Boveris, L.B. Valdez, T. Zaobornyj, J. Bustamante, Mitochondrial metabolic states regulate nitric oxide and hydrogen peroxide diffusion to the cytosol, Biochim Biophys Acta. 1757 (2006) 535–542. http://www.ncbi.nlm.nih.gov/entrez/query.fcgi?cmd=Retrieve&db=PubMed&dopt=Citation&list_uids=16615992.

[16] L.B. Valdez, T. Zaobornyj, A. Boveris, Mitochondrial metabolic states and membrane potential modulate mtNOS activity, Biochim Biophys Acta. 1757 (2006) 166–172. http://www.ncbi.nlm.nih.gov/entrez/query.fcgi?cmd=Retrieve&db=PubMed&dopt=Citation&list_uids=16624252.

[17] F. Yin, H. Sancheti, E. Cadenas, Mitochondrial Thiols in the Regulation of Cell Death Pathways, Antioxidants & Redox Signaling. 17 (2012) 1714–1727. doi:10.1089/ars.2012.4639.

[18] A. Boveris, L. Costa, E. Cadenas, The mitochondrial production of oxygen radicals and cellular aging, in: C. E, P. L (Eds.), Understanding the Process of Aging: The Roles of Mitochondria, Free Radicals, and Antioxidants, New York, Dekker, 1999: pp. 1–16.

[19] S. Alvarez, L.B. Valdez, T. Zaobornyj, A. Boveris, Oxygen dependence of mitochondrial nitric oxide synthase activity, Biochem Biophys Res Commun. 305 (2003) 771–775. http://www.ncbi.nlm.nih.gov/entrez/query.fcgi?cmd=Retrieve&db=PubMed&dopt=Citation&list_uids=12763059.

[20] A. Boveris, S.L. Arnaiz, J. Bustamante, S. Alvarez, L. Valdez, A.D. Boveris, et al., Pharmacological regulation of mitochondrial nitric oxide synthase., Methods in Enzymology. 359 (2002) 328–39. http://www.ncbi.nlm.nih.gov/pubmed/12481584 (accessed November 4, 2015).

[21] L.B. Valdez, T. Zaobornyj, S. Alvarez, J. Bustamante, L.E. Costa, A. Boveris, Heart mitochondrial nitric oxide synthase. Effects of hypoxia and aging, Mol Aspects Med. 25 (2004) 49–59.

http://www.ncbi.nlm.nih.gov/entrez/query.fcgi?cmd=Retrieve&db=PubMed&dopt=Citation&list_uids=15051316.

[22] G.F. Gonzales, F.A. Chung, S. Miranda, L.B. Valdez, T. Zaobornyj, J. Bustamante, et al., Heart mitochondrial nitric oxide synthase is upregulated in male rats exposed to high altitude (4,340 m)., American Journal of Physiology. Heart and Circulatory Physiology. 288 (2005) H2568–73. doi:10.1152/ajpheart.00812.2004.

[23] T. Zaobornyj, L.B. Valdez, P. La Padula, L.E. Costa, A. Boveris, Effect of sustained hypobaric hypoxia during maturation and aging on rat myocardium. II. mtNOS activity, J Appl Physiol (1985). 98 (2005) 2370–2375. http://www.ncbi.nlm.nih.gov/entrez/query.fcgi?cmd=Retrieve&db=PubMed&dopt=Citation&list_uids=15705730.

[24] L.B. Valdez, T. Zaobornyj, S. Bombicino, D.E. Iglesias, A. Boveris, M. Donato, et al., Complex I syndrome in myocardial stunning and the effect of adenosine, Free Radical Biology and Medicine. 51 (2011) 1203–1212.

[25] V. Vanasco, N.D. Magnani, M.C. Cimolai, L.B. Valdez, P. Evelson, A. Boveris, et al., Endotoxemia impairs heart mitochondrial function by decreasing electron transfer, ATP synthesis and ATP content without affecting membrane potential, J Bioenerg Biomembr. 44 (2012) 243–252. http://www.ncbi.nlm.nih.gov/entrez/query.fcgi?cmd=Retrieve&db=PubMed&dopt=Citation&list_uids=22426814.

[26] M.W. Cleeter, J.M. Cooper, V.M. Darley-Usmar, S. Moncada, A.H. Schapira, Reversible inhibition of cytochrome c oxidase, the terminal enzyme of the mitochondrial respiratory chain, by nitric oxide. Implications for neurodegenerative diseases, FEBS Lett. 345 (1994) 50–54. http://www.ncbi.nlm.nih.gov/entrez/query.fcgi?cmd=Retrieve&db=PubMed&dopt=Citation&list_uids=8194600.

[27] G.C. Brown, C.E. Cooper, Nanomolar concentrations of nitric oxide reversibly inhibit synaptosomal respiration by competing with oxygen at cytochrome oxidase, FEBS Lett. 356 (1994) 295–298. http://www.ncbi.nlm.nih.gov/entrez/query.fcgi?cmd=Retrieve&db=PubMed&dopt=Citation&list_uids=7805858.

[28] Y. Takehara, H. Nakahara, Y. Inai, M. Yabuki, K. Hamazaki, T. Yoshioka, et al., Oxygen-dependent reversible inhibition of mitochondrial respiration by nitric oxide., Cell Structure and Function. 21 (1996) 251–8. http://www.ncbi.nlm.nih.gov/pubmed/8906361 (accessed March 1, 2017).

[29] J.J. Poderoso, J.G. Peralta, C.L. Lisdero, M.C. Carreras, M. Radisic, F. Schopfer, et al., Nitric oxide regulates oxygen uptake and hydrogen peroxide release by the isolated beating rat heart, Am J Physiol. 274 (1998) C112–9. http://www.ncbi.nlm.nih.gov/entrez/query.fcgi?cmd=Retrieve&db=PubMed&dopt=Citation&list_uids=9458719.

[30] D.E. Iglesias, S.S. Bombicino, L.B. Valdez, A. Boveris, Nitric oxide interacts with mitochondrial complex III producing antimycin-like effects., Free Radical Biology & Medicine. 89 (2015) 602–13. doi:10.1016/j.freeradbiomed.2015.08.024.

[31] T. Persichini, V. Mazzone, F. Polticelli, S. Moreno, G. Venturini, E. Clementi, et al., Mitochondrial type I nitric oxide synthase physically interacts with cytochrome c oxidase, Neurosci Lett. 384 (2005) 254–259. http://www.ncbi.nlm.nih.gov/entrez/query.fcgi?cmd=Retrieve&db=PubMed&dopt=Citation&list_uids=15923083.

[32] M.C. Franco, V.G. Antico Arciuch, J.G. Peralta, S. Galli, D. Levisman, L.M. Lopez, et al., Hypothyroid phenotype is contributed by mitochondrial complex I inactivation due to translocated neuronal nitric-oxide synthase, J Biol Chem. 281 (2006) 4779–4786. http://www.ncbi.nlm.nih.gov/entrez/query.fcgi?cmd=Retrieve&db=PubMed&dopt=Citation&list_uids=16361261.

[33] M.S. Parihar, A. Parihar, F.A. Villamena, P.S. Vaccaro, P. Ghafourifar, Inactivation of mitochondrial respiratory chain complex I leads mitochondrial nitric oxide synthase to become pro-oxidative, Biochem Biophys Res Commun. 367 (2008) 761–767. http://www.ncbi.nlm.nih.gov/entrez/query.fcgi?cmd=Retrieve&db=PubMed&dopt=Citation&list_uids=18191636.

[34] S.S. Bombicino, D.E. Iglesias, T. Zaobornyj, A. Boveris, L.B. Valdez, Mitochondrial nitric oxide production supported by reverse electron transfer, Archives of Biochemistry and Biophysics. 607 (2016) 8–19. doi:10.1016/j.abb.2016.08.010.

[35] L. Valdez, S. Bombicino, D. Iglesias, I. Rukavina Mikusic, V. D'Annunzio, Mitochondrial complex I inactivation after ischemia-reperfusion in the stunned heart, in: R. Gelpi, A. Boveris, J. Poderoso (Eds.), Advances in Biochemistry in Health and Disease. Biochemistry of Oxidative Stress: Physiopathology and Clinical Aspects, Springer, New York, USA, 2016: pp. 245–257.

[36] C.S. Boyd, E. Cadenas, Nitric Oxide and Cell Signaling Pathways in Mitochondrial-Dependent Apoptosis, Biological Chemistry. 383 (2002) 411–23. doi:10.1515/BC.2002.045.

[37] S.L. Wynia-Smith, B.C. Smith, Nitrosothiol formation and S-nitrosation signaling through nitric oxide synthases, Nitric Oxide. 63 (2017) 52–60. doi:10.1016/j.niox.2016.10.001.

[38] L.B. Valdez, S. Alvarez, S.L. Arnaiz, F. Schopfer, M.C. Carreras, J.J. Poderoso, et al., Reactions of peroxynitrite in the mitochondrial matrix, Free Radic Biol Med. 29 (2000) 349–356. http://www.ncbi.nlm.nih.gov/entrez/query.fcgi?cmd=Retrieve&db=PubMed&dopt=Citation&list_uids=11035264.

[39] R. Radi, A. Cassina, R. Hodara, C. Quijano, L. Castro, Peroxynitrite reactions and formation in mitochondria., Free Radical Biology & Medicine. 33 (2002) 1451–64. http://www.ncbi.nlm.nih.gov/pubmed/12446202 (accessed March 1, 2017).

[40] P. Pacher, J.S. Beckman, L. Liaudet, Nitric oxide and peroxynitrite in health and disease., Physiological Reviews. 87 (2007) 315–424. doi:10.1152/physrev.00029.2006.

[41] D.P. Jones, H. Sies, The Redox Code., Antioxidants & Redox Signaling. 23 (2015) 734–46. doi:10.1089/ars.2015.6247.

[42] H. Sies, Oxidative stress: a concept in redox biology and medicine, Redox Biology. 4 (2015) 180–183. doi:10.1016/j.redox.2015.01.002.

[43] F. Yin, A. Boveris, E. Cadenas, Mitochondrial energy metabolism and redox signaling in brain aging and neurodegeneration., Antioxidants & Redox Signaling. 20 (2014) 353–71. doi:10.1089/ars.2012.4774.

[44] F. Yin, E. Cadenas, Mitochondria: The Cellular Hub of the Dynamic Coordinated Network, Antioxidants & Redox Signaling. 22 (2015) 961–964. doi:10.1089/ars.2015.6313.

[45] H. Sies, Hydrogen peroxide as a central redox signaling molecule in physiological oxidative stress: Oxidative eustress, Redox Biology. 11 (2017) 613–619. doi:10.1016/j.redox.2016.12.035.

[46] F. Antunes, E. Cadenas, Estimation of H2O2 gradients across biomembranes., FEBS Letters. 475 (2000) 121–6. http://www.ncbi.nlm.nih.gov/pubmed/10858501 (accessed June 28, 2017).

[47] H.S. Marinho, L. Cyrne, E. Cadenas, F. Antunes, The Cellular Steady-State of H2O2, in: Methods in Enzymology, 2013: pp. 3–19. doi:10.1016/B978-0-12-405882-8.00001-5.

[48] D. Booth, B. Enyedi, M. Geiszt, P. V?rnai, G. Hajn?czky, Redox Nanodomains Are Induced by and Control Calcium Signaling at the ER-Mitochondrial Interface, Molecular Cell. 63 (2016) 240–248. doi:10.1016/j.molcel.2016.05.040.

[49] M.N. Gadaleta, G. Rainaldi, A.M. Lezza, F. Milella, F. Fracasso, P. Cantatore, Mitochondrial DNA copy number and mitochondrial DNA deletion in adult and senescent rats., Mutation Research. 275 (1992) 181–93. http://www.ncbi.nlm.nih.gov/pubmed/1383760 (accessed September 12, 2015).

[50] H.C. Lee, P.H. Yin, C.Y. Lu, C.W. Chi, Y.H. Wei, Increase of mitochondria and mitochondrial DNA in response to oxidative stress in human cells., The Biochemical Journal. 348 Pt 2 (2000) 425–432.

[51] E. Nisoli, E. Clementi, C. Paolucci, V. Cozzi, C. Tonello, C. Sciorati, et al., Mitochondrial biogenesis in mammals: the role of endogenous nitric oxide., Science (New York, N.Y.). 299 (2003) 896–9. doi:10.1126/science.1079368.

[52] E. Clementi, E. Nisoli, Nitric oxide and mitochondrial biogenesis: a key to long-term regulation of cellular metabolism., Comparative Biochemistry and Physiology. Part A, Molecular & Integrative Physiology. 142 (2005) 102–10. doi:10.1016/j.cbpb.2005.04.022.

[53] A.P. Rolo, C.M. Palmeira, Diabetes and mitochondrial function: Role of hyperglycemia and oxidative stress, Toxicology and Applied Pharmacology. 212 (2006) 167–178. doi:10.1016/j.taap.2006.01.003.

[54] C.G. Tocchetti, B.A. Stanley, V. Sivakumaran, D. Bedja, B. O'Rourke, N. Paolocci, et al., Impaired mitochondrial energy supply coupled to increased H_2O_2 emission under energy/redox stress leads to myocardial dysfunction during Type I diabetes, Clinical Science. 129 (2015) 561–574. doi:10.1042/CS20150204.

[55] S. Boudina, E.D. Abel, Diabetic cardiomyopathy revisited., Circulation. 115 (2007) 3213–23. doi:10.1161/CIRCULATIONAHA.106.679597.

[56] L. Cai, Suppression of nitrative damage by metallothionein in diabetic heart contributes to the prevention of cardiomyopathy., Free Radical Biology & Medicine. 41 (2006) 851–61. doi:10.1016/j.freeradbiomed.2006.06.007.

[57] Z. Chen, B. Siu, Y.S. Ho, R. Vincent, C.C. Chua, R.C. Hamdy, et al., Overexpression of MnSOD protects against myocardial ischemia/reperfusion injury in transgenic mice., Journal of Molecular and Cellular Cardiology. 30 (1998) 2281–9. doi:10.1006/jmcc.1998.0789.

[58] S.S. Bombicino, D.E. Iglesias, I.A.R. Mikusic, V. D'Annunzio, R.J. Gelpi, A. Boveris, et al., Diabetes impairs heart mitochondrial function without changes in resting cardiac performance, The International Journal of Biochemistry & Cell Biology. 81 (2016) 335–345. doi:10.1016/j.biocel.2016.09.018.

[59] A.A. Rossini, A.A. Like, W.L. Chick, M.C. Appel, G.F. Cahill, Studies of streptozotocin-induced insulitis and diabetes., Proceedings of the National Academy of Sciences of the United States of America. 74 (1977) 2485–9. http://www.ncbi.nlm.nih.gov/pubmed/142253 (accessed March 1, 2017).

[60] C. Li, Q. Zhang, M. Li, J. Zhang, P. Yu, D. Yu, Attenuation of myocardial apoptosis by alpha-lipoic acid through suppression of mitochondrial oxidative stress to reduce diabetic cardiomyopathy., Chinese Medical Journal. 122 (2009) 2580–6. http://www.ncbi.nlm.nih.gov/pubmed/19951573 (accessed March 1, 2017).

[61] I.I. Joffe, K.E. Travers, C.L. Perreault-Micale, T. Hampton, S.E. Katz, J.P. Morgan, et al., Abnormal cardiac function in the streptozotocin-induced non-insulin-dependent diabetic rat: noninvasive assessment with doppler echocardiography and contribution of the nitric oxide pathway., Journal of the American College of Cardiology. 34 (1999) 2111–9. http://www.ncbi.nlm.nih.gov/pubmed/10588232 (accessed March 1, 2017).

[62] L. Mela, S. Seitz, Isolation of mitochondria with emphasis on heart mitochondria from small amounts of tissue., Methods in Enzymology. 55 (1979) 39–46. http://www.ncbi.nlm.nih.gov/pubmed/459851 (accessed March 1, 2017).

[63] O.H. Lowry, N.J. Rosebrough, A.L. Farr, R.J. Randall, Protein measurement with the Folin phenol reagent., The Journal of Biological Chemistry. 193 (1951) 265–75. http://www.ncbi.nlm.nih.gov/pubmed/14907713 (accessed March 1, 2017).

[64] A. Boveris, Determination of the production of superoxide radicals and hydrogen peroxide in mitochondria, Methods Enzymol. 105 (1984) 429–435. http://www.ncbi.nlm.nih.gov/entrez/query.fcgi?cmd=Retrieve&db=PubMed&dopt=Citation&list_uids=6328196.

[65] M.E. Murphy, E. Noack, Nitric oxide assay using hemoglobin method, Methods Enzymol. 233 (1994) 240–250.

[66] J. Bustamante, G. Bersier, R.A. Badin, C. Cymeryng, A. Parodi, A. Boveris, Sequential NO production by mitochondria and endoplasmic reticulum during induced apoptosis, Nitric Oxide. 6 (2002) 333–341.

http://www.ncbi.nlm.nih.gov/entrez/query.fcgi?cmd=Retrieve&db=PubMed&dopt=Citation&list_uids=12009851.

[67] F.R. Leach, J.J. Webster, Commercially available firefly luciferase reagents., Methods in Enzymology. 133 (1986) 51–70. http://www.ncbi.nlm.nih.gov/pubmed/3821551 (accessed March 1, 2017).

[68] B. Drew, C. Leeuwenburgh, Method for measuring ATP production in isolated mitochondria: ATP production in brain and liver mitochondria of Fischer-344 rats with age and caloric restriction., American Journal of Physiology. Regulatory, Integrative and Comparative Physiology. 285 (2003) R1259–67. doi:10.1152/ajpregu.00264.2003.

[69] T. Marchini, N. Magnani, V. D'Annunzio, D. Tasat, R.J. Gelpi, S. Alvarez, et al., Impaired cardiac mitochondrial function and contractile reserve following an acute exposure to environmental particulate matter, Biochimica et Biophysica Acta (BBA) - General Subjects. 1830 (2013) 2545–2552. doi:10.1016/j.bbagen.2012.11.012.

[70] J.M. Petit, A. Maftah, M.H. Ratinaud, R. Julien, 10N-nonyl acridine orange interacts with cardiolipin and allows the quantification of this phospholipid in isolated mitochondria., European Journal of Biochemistry. 209 (1992) 267–73. http://www.ncbi.nlm.nih.gov/pubmed/1396703 (accessed March 1, 2017).

[71] A. Czerniczyniec, A.G. Karadayian, J. Bustamante, R.A. Cutrera, S. Lores-Arnaiz, Paraquat induces behavioral changes and cortical and striatal mitochondrial dysfunction., Free Radical Biology & Medicine. 51 (2011) 1428–36. doi:10.1016/j.freeradbiomed.2011.06.034.

[72] L.E. Costa, A. Boveris, O.R. Koch, A.C. Taquini, Liver and heart mitochondria in rats submitted to chronic hypobaric hypoxia, Am J Physiol. 255 (1988) C123–9. http://www.ncbi.nlm.nih.gov/entrez/query.fcgi?cmd=Retrieve&db=PubMed&dopt=Citation&list_uids=2839034.

[73] A. Navarro, A. Boveris, M.J. Bandez, M.J. Sanchez-Pino, C. Gomez, G. Muntane, et al., Human brain cortex: mitochondrial oxidative damage and adaptive response in Parkinson disease and in dementia with Lewy bodies, Free Radic Biol Med. 46 (2009) 1574–1580. http://www.ncbi.nlm.nih.gov/entrez/query.fcgi?cmd=Retrieve&db=PubMed&dopt=Citation&list_uids=19298851.

[74] A.A. Caro, M. Bell, S. Ejiofor, G. Zurcher, D.R. Petersen, M.J.J. Ronis, N-acetylcysteine inhibits the up-regulation of mitochondrial biogenesis genes in livers from rats fed ethanol chronically., Alcoholism, Clinical and Experimental Research. 38 (2014) 2896–906. doi:10.1111/acer.12576.

[75] T. Yonetani, G.S. Ray, Studies on cytochrome oxidase. VI. Kinetics of the aerobic oxidation of ferrocytochrome c by cytochrome oxidase., The Journal of Biological Chemistry. 240 (1965) 3392–8. http://www.ncbi.nlm.nih.gov/pubmed/14321378 (accessed March 1, 2017).

[76] T. Yonetani, Cytochrome oxidase: beef heart., Meth Enzymol. 10 (1967) 332–335. http://dx.doi.org/10.1016/0076-6879(67)10062-1.

[77] D.M. Medeiros, Assessing mitochondria biogenesis., Methods (San Diego, Calif.). 46 (2008) 288–94. doi:10.1016/j.ymeth.2008.09.026.

[78] E. Weibel, W. Stäubli, H. Gnägi, H. FA, Correlated morphometric and biochemical studies on the liver cell. I. Morphometric model, stereologic methods, and normal morphometric data for rat liver, J. Cell. Biol. 42 (1969) 68–91.

[79] Z. Wu, P. Puigserver, U. Andersson, C. Zhang, G. Adelmant, V. Mootha, et al., Mechanisms Controlling Mitochondrial Biogenesis and Respiration through the Thermogenic Coactivator PGC-1, Cell. 98 (1999) 115–124. doi:10.1016/S0092-8674(00)80611-X.

[80] P. Puigserver, Z. Wu, C.W. Park, R. Graves, M. Wright, B.M. Spiegelman, A cold-inducible coactivator of nuclear receptors linked to adaptive thermogenesis., Cell. 92 (1998) 829–39. http://www.ncbi.nlm.nih.gov/pubmed/9529258 (accessed March 1, 2017).

[81] J.J. Lehman, P.M. Barger, A. Kovacs, J.E. Saffitz, D.M. Medeiros, D.P. Kelly, Peroxisome proliferator-activated receptor gamma coactivator-1 promotes cardiac mitochondrial biogenesis., The Journal of Clinical Investigation. 106 (2000) 847–56. doi:10.1172/JCI10268.

[82] I. Irrcher, V. Ljubicic, D.A. Hood, Interactions between ROS and AMP kinase activity in the regulation of PGC-1 transcription in skeletal muscle cells, AJP: Cell Physiology. 296 (2009) C116–C123. doi:10.1152/ajpcell.00267.2007.

[83] C. Ling, P. Poulsen, E. Carlsson, M. Ridderstråle, P. Almgren, J. Wojtaszewski, et al., Multiple environmental and genetic factors influence skeletal muscle PGC-1a and PGC-1B gene expression in twins, Journal of Clinical Investigation. 114 (2004) 1518–1526. doi:10.1172/JCI200421889.1518.

[84] L.B. Valdez, A. Boveris, Nitric oxide and superoxide radical production by human mononuclear leukocytes, Antioxid Redox Signal. 3 (2001) 505–513. http://www.ncbi.nlm.nih.gov/entrez/query.fcgi?cmd=Retrieve&db=PubMed&dopt=Citation&list_uids=11491661.

[85] R. Kissner, T. Nauser, P. Bugnon, P.G. Lye, W.H. Koppenol, Formation and properties of peroxynitrite as studied by laser flash photolysis, high-pressure stopped-flow technique, and pulse radiolysis., Chemical Research in Toxicology. 10 (1997) 1285–92. doi:10.1021/tx970160x.

[86] H. Bugger, E.D. Abel, Mitochondria in the diabetic heart, Cardiovascular Research. 88 (2010) 229–240. doi:10.1093/cvr/cvq239.

[87] L.K. Russell, Cardiac-Specific Induction of the Transcriptional Coactivator Peroxisome Proliferator-Activated Receptor Coactivator-1 Promotes Mitochondrial Biogenesis and Reversible Cardiomyopathy in a Developmental Stage-Dependent Manner, Circulation Research. 94 (2004) 525–533. doi:10.1161/01.RES.0000117088.36577.EB.

HIGHLIGHTS

- Mitochondrial biogenesis is triggered in heart of STZ-induced diabetic rats
- Mitochondrial NO, $ONOO^-$ and H_2O_2 productions are increased in heart of diabetic rats
- Heart mitochondrial $[O_2^{\bullet -}]_{ss}$ and $[NO]_{ss}$ are higher in diabetic than in control rats
- Changes in membrane potential and ATP synthesis lead to energetic-state imbalances
- NO, H_2O_2 and ATP are signaling molecules involved in mitochondrial biogenesis

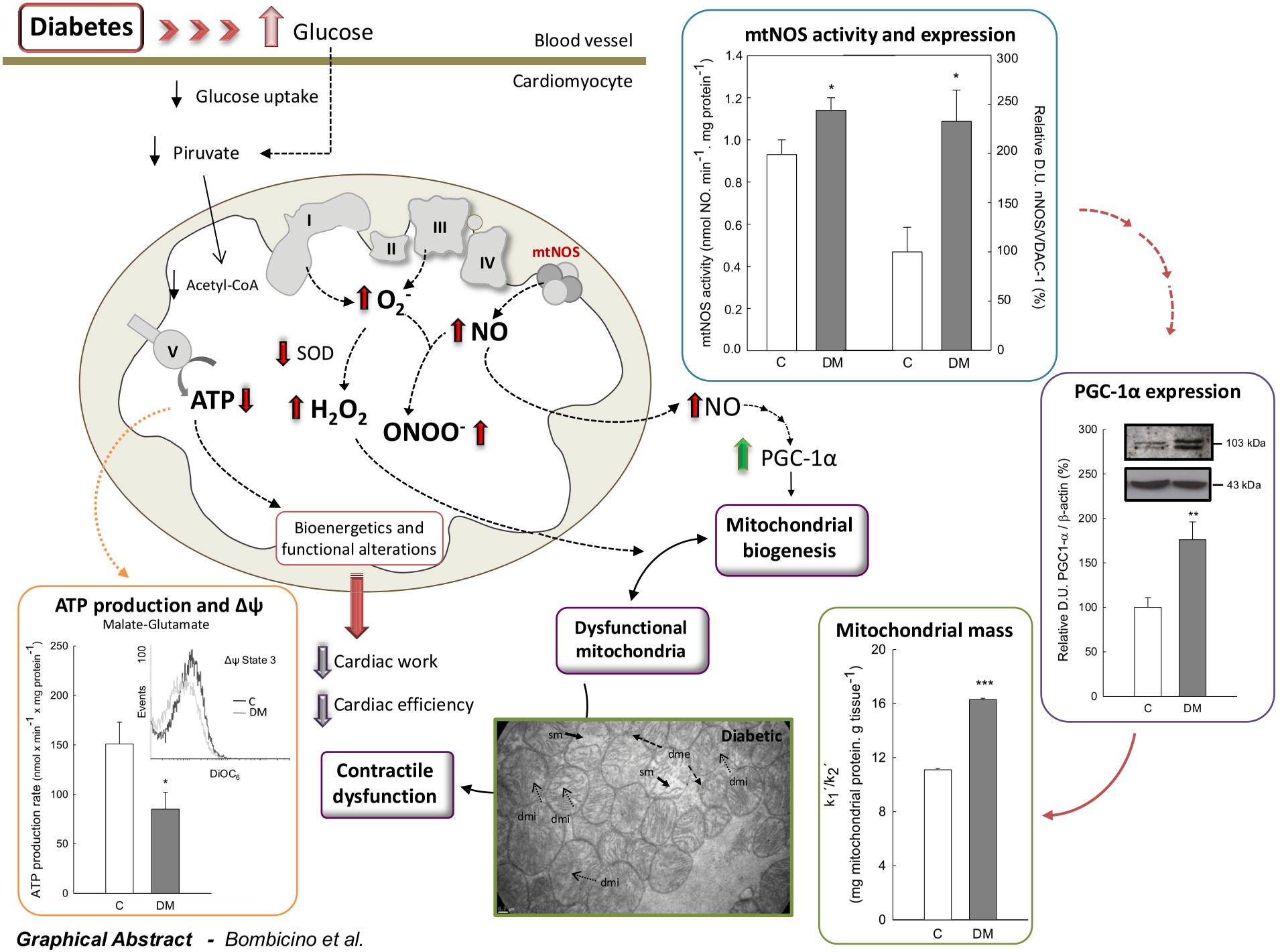

Graphical Abstract - *Bombicino et al.*